Int. J. Heat Mass Transfer. Vol. 28, No. 1, pp. 207–217, 1985
Printed in Great Britain

0017–9310/85 $3.00 + 0.00

Laminar, mixed convection heat transfer for flow between horizontal parallel plates with asymmetric heating

D. G. OSBORNE and F. P. INCROPERA
Heat Transfer Laboratory, School of Mechanical Engineering, Purdue University, W. Lafayette, IN 47907, U.S.A.

(*Received* 30 *January* 1984 *and in revised form* 30 *May* 1984)

Abstract—An experimental study has been conducted to determine hydrodynamic and thermal conditions in laminar water flow between horizontal parallel plates with uniform, asymmetric heat fluxes. Flow visualization and temperature measurements reveal the existence of a buoyancy driven flow which strongly influences bottom plate conditions but has a weak influence on top plate conditions. Heat transfer at the top plate is dominated by forced convection, while heat transfer at the bottom plate is characterized by mixed convection and can be correlated in terms of the parameter $Ra_{H,q}^{3/4}/Gz_H$ for top to bottom heat fluxes less than 2. For the range of heat fluxes considered, top and bottom plate flow conditions are independent of the heat flux at the opposite plate.

1. INTRODUCTION

IN RECENT years there has been considerable interest in the effects of buoyancy on laminar internal flow. In the case of horizontal channels, buoyancy forces induce a secondary flow which can reduce the thermal entry length, enhance heat transfer, and promote early transition to turbulence. Experimental [1–5] and theoretical [6–11] studies of laminar mixed convection in horizontal circular tubes have revealed heat transfer coefficients which are as much as four times larger than those associated with pure forced convection. The mixed convection regime has been delineated and general heat transfer correlations have been proposed. Secondary flows have been shown to be in the form of longitudinal rolls, and the effects of asymmetric heating on flow and heat transfer have been determined.

Laminar mixed convection flow and heat transfer in horizontal, rectangular channels has also been studied. Experiments have revealed the existence of longitudinal rolls and heat transfer enhancement up to five times that associated with forced convection [12–17]. Enhancement is larger for the fully developed than for the entrance region, and the length of the entry region decreases with increasing buoyancy. These trends have been predicted for the entrance and fully developed regions of flow between parallel plates and through channels of finite aspect ratio [18–24].

The present study was motivated by the fact that few experiments have been performed to determine the effects of buoyancy on flow in a horizontal channel which is heated from above and below. While heating from below induces a buoyancy flow which enhances heat transfer, heating from above acts to stratify the flow and hence to inhibit heat transfer. A major objective of the study has therefore been to determine the effects of thermal destabilization and thermal stratification on heat transfer at both the top and bottom surfaces. Additional objectives have been to observe and correlate onset of the buoyancy flow and to correlate heat transfer results. Experiments have been performed for water flow in a horizontal channel and have involved flow visualization as well as temperature and heat transfer measurements.

2. EXPERIMENTAL PROCEDURES

Experiments were performed using the water channel of Fig. 1. The channel is 0.305 m wide and has developing and test sections which are 1.05 m and 0.97 m long, respectively. Two heights (20 mm and 60 mm) were considered. All channel walls were constructed from 12.7 mm Plexiglas, except the top and bottom of the test section, which were fabricated from 9.5 mm aluminum plate.

Test section surface temperature measurements were obtained from 19 thermocouples imbedded in the bottom plate and 23 thermocouples in the top plate. Beginning at $z = 51$ mm, plate temperatures were measured at 111 mm intervals along the midline and at selected stations off the midline. Vertical temperature distributions in the water were determined using thermocouples mounted to a traversing mechanism. By coupling a reversible motor to a potentiometer, the thermocouples could be traversed at 10 mm/min and the temperature and position outputs measured on an x–y recorder.

A uniform heat flux was maintained at the top and bottom surfaces of the test section by Electrofilm patch heaters which were joined to the side of the aluminum plate removed from the water. The fluxes were independently controlled and could be varied over the range from 0 to 6000 W/m^2. The outer surfaces of the heaters were insulated, and heat loss to the surroundings was estimated to be less than 1%.

NOMENCLATURE

c_p	specific heat
g	acceleration due to gravity
Gr_H	Grashof number, $g\beta(T_{bp}-T_m)H^3/v^2$
$Gr_{H,q}$	Grashof number, $g\beta q_b H^4/kv^2$
Gz_H	Graetz number, $(H/z)Re_H Pr$
H	channel height
h	local convection heat transfer coefficient
k	thermal conductivity
Nu_H	Nusselt number, hH/k
Pr	Prandtl number
q	heat transfer rate per unit area
Ra_H	Rayleigh number, $Gr_H Pr$
$Ra_{H,q}$	Rayleigh number, $Gr_{H,q}Pr$
Re_H	Reynolds number, $w_m H/v$
T	temperature
w	longitudinal velocity
y	vertical distance from bottom plate
z	longitudinal distance from test section entrance.

Greek symbols

β	thermal expansion coefficient
ρ	density
v	kinematic viscosity.

Subscripts

b	bottom plate
F	pure forced convection
H	based on plate height
m	mean value
N	pure natural or free convection
p	plate condition
q	based on bottom plate heat flux, q_b
t	top plate.

Departures from a uniform surface heat flux condition are due to longitudinal conduction in the aluminum plate and to heat loss from the plate to the Plexiglas developing section at the leading edge. Including these effects in a two-dimensional, steady-state conduction analysis of the plate, the deviation in the uniform flux condition was estimated to be less than 10% at the first measurement station ($z = 51$ mm) and less than 3% at all subsequent stations.

A flowmeter, valve and pump arrangement were used to control and measure the mean velocity of water flow through the test section and a flow straightener was used to achieve a uniform velocity profile at the inlet to the developing section. Hydrodynamic development within this section is sufficient to insure fully developed conditions at $z = 0$ for $H = 20$ mm but is not quite sufficient for $H = 60$ mm [25]. However, because the effect of velocity profile variations on heat transfer is small for moderate to large Pr [26], it is reasonable to assume thermal entry length conditions (a fully developed velocity profile at $z = 0$) for all conditions of this study.

The flow was visualized through the side walls by using both dye-injection and shadowgraph techniques. Both methods reveal the existence of thermals rising from the heated bottom plate, as well as the extent to which the flow becomes mixed. Since the shadowgraph is a recording of light passing through the channel, it is a two-dimensional technique which provides an indication of spanwise averaged conditions.

At the bottom and top surfaces, convection coefficients are determined from

$$q = h(T_p - T_m) \tag{1}$$

where the heat flux and plate temperature are measured quantities and the mean temperature is determined from the energy balance

$$T_m(z) = T_m(z=0) + \frac{(q_t + q_b)z}{w_m H \rho c_p}. \tag{2}$$

Top and bottom heat transfer coefficients were calculated at the eight longitudinal stations corresponding to measurement of T_p, and results were correlated in terms of the Nusselt (Nu_H), Reynolds (Re_H), and Grashof ($Gr_{H,q}$) numbers. All properties were evaluated at the local mean temperature, $T_m(z)$. Experiments were performed for 65 different operating conditions for which $0 \leqslant (q_b, q_t) \leqslant 6000$ W/m^2 and $3 \leqslant w_m \leqslant 60$ mm/s. With bottom heating, Grashof numbers were in the range $4.3 \times 10^5 \leqslant Gr_{H,q} \leqslant 4.2$

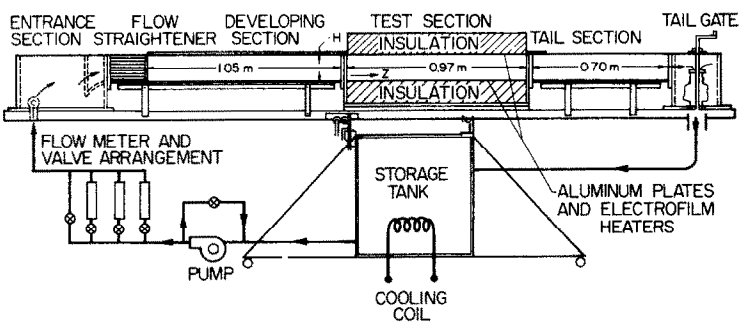

FIG. 1. Schematic of flow channel.

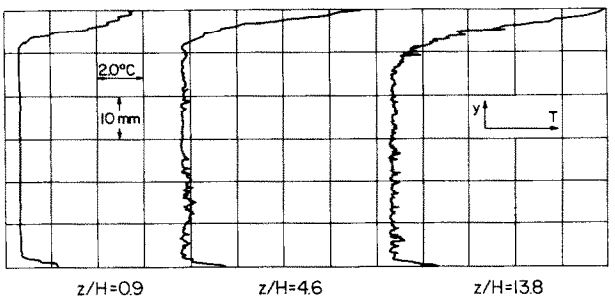

FIG. 2. Vertical temperature distributions for $q_b = q_t = 1000$ W/m^2, $w_m = 10$ mm/s, $H = 60$ mm, $Re_H = 650$ and $Gr_{H,q} = 7.0 \times 10^7$.

$\times 10^8$. All but one of the experiments were performed for Reynolds numbers in the range $65 \leqslant Re_H \leqslant 1300$, providing for laminar flow conditions at $z = 0$.

All plate temperature measurements were made along the midline in order to minimize the influence of side wall effects and to maximize applicability of the results to infinite parallel plates. Although regular spanwise temperature variations have been observed for air flow in a channel and have been associated with the formation of longitudinal rolls [12, 14], no such rolls were observed in this study. Moreover, plate temperatures varied by less than 1°C in the spanwise direction, with no consistent trend in the variations.

Using established procedures [27], uncertainties in Nu_H were estimated to be in the range from 6% to 30%. The larger uncertainties are due to small temperature differences ($T_p - T_m$) associated with the low heat flux experiments. Uncertainties in $Gr_{H,q}$ and Re_H are in the ranges 8–21% and 2–12%, respectively.

3. RESULTS

3.1 *Temperature distributions and flow visualization*

For pure forced convection between horizontal parallel plates, equivalent conditions are associated with each plate. However, if free convection is significant, conditions are asymmetrical, with the degree of asymmetry depending upon the relative influence of free and forced convection effects. This behavior is demonstrated by the asymmetrical temperature distributions of Fig. 2. As early as $z/H = 0.9$, buoyancy induced flow originating from the bottom plate causes T_b to be significantly less than T_t. Further downstream, the buoyancy driven flow becomes random, and fluctuations are associated with the temperature distributions. This behavior is in sharp contrast to that of Fig. 3, for which there is no buoyancy flow and the temperature distributions are smooth. The distributions are typical of laminar, forced convection, thermal boundary layer development, as T_t increases markedly with increasing z. Similar behavior characterizes the top plate boundary layer of Fig. 2. Although buoyancy induced mixing becomes intense through most of the channel, penetration to the top plate is inhibited by thermal stratification in the top boundary layer. The effect of bottom heating on conditions in this boundary layer is small, as T_t continues to increase with increasing z. The smooth portion of the temperature profile at $z/H = 4.6$ in Fig. 2 is attributed to the random nature of the buoyancy driven flow (in inlet regions of the channel, vertical penetration of this flow has been observed to vary with time).

The effect of increasing the bottom plate heat flux is to increase the destabilizing temperature gradient in the bottom boundary layer and to enhance the buoyancy induced flow. As shown in Fig. 4, increasing q_b has the effect of increasing the amplitude and frequency of the temperature fluctuations and advancing vertical penetration of the fluctuations. Similar results are associated with a reduction in w_m, and except for conditions in the top boundary layer, there is little effect of increasing q_t.

A composite of dye-injection results is shown in Fig.

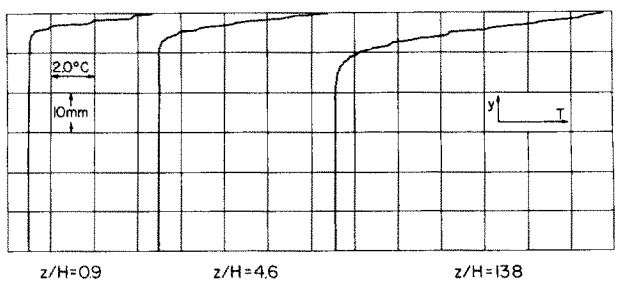

FIG. 3. Vertical temperature distributions for $q_b = 0$, $q_t = 1000$ W/m^2, $w_m = 10$ mm/s, $H = 60$ mm and $Re_H = 650$.

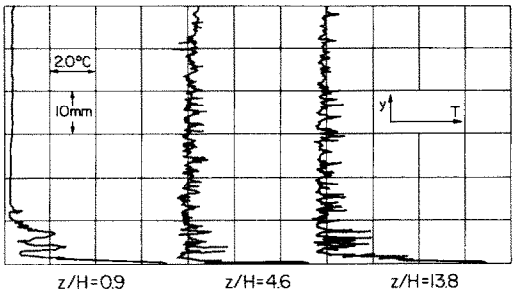

FIG. 4. Vertical temperature distributions for $q_b = 6000$ W/m^2, $q_t = 0$, $w_m = 10$ mm/s, $H = 60$ mm, $Re_H = 650$, $Gr_{H,q} = 4.2 \times 10^8$.

5. The existence of a buoyancy induced flow is revealed by vertical penetration of the dye, which is injected parallel to the flow at $y = z = 0$. Additional photographs taken for each of the conditions of the figure reveal that vertical penetration varies with time (the secondary flow is random). Contrasting Figs 5(a) and 5(b), increasing Re_H is seen to suppress the secondary flow and to increase the longitudinal distance required for penetration to a fixed height. Decreasing the channel height, and hence the Grashof number, for a fixed Reynolds number also suppresses free convection effects, as shown by Figs 5(a) and 5(d).

Onset of the buoyancy induced flow, which leads to ascension of the dye, moves from approximately $z/H = 0.3$ for $H = 60$ mm in Fig. 5(a) to approximately $z/H = 6.3$ for $H = 20$ mm in Fig. 5(d). The result is due to an increase in the effects of shear relative to buoyancy forces. The effect of increasing the Grashof number is seen from Figs 5(a) and 5(c). Secondary flow is enhanced and the longitudinal station for which this flow penetrates to a fixed height is advanced. In Fig. 5(c) the flow has penetrated to the top plate at $z/H \approx 2.7$ and the mixing pattern is suggestive of turbulent free convection.

The effect of top plate heating on flow which is induced by heating from below is shown in Figs 5(e) and (5f). In 5(c) the secondary flow has penetrated to the top, while in 5(f) penetration has been restricted by the stable thermal boundary layer. However, this layer does not appear to significantly influence secondary flow in the core of the channel or near the bottom plate. The results are consistent with those of Figs 2–4 and suggest that, for the conditions of this study, q_t has a negligible effect on flow and thermal conditions at the bottom plate.

Representative results from the shadowgraph technique are shown in Figs 6–8. The effect which increasing Re_H has on inhibiting vertical penetration of

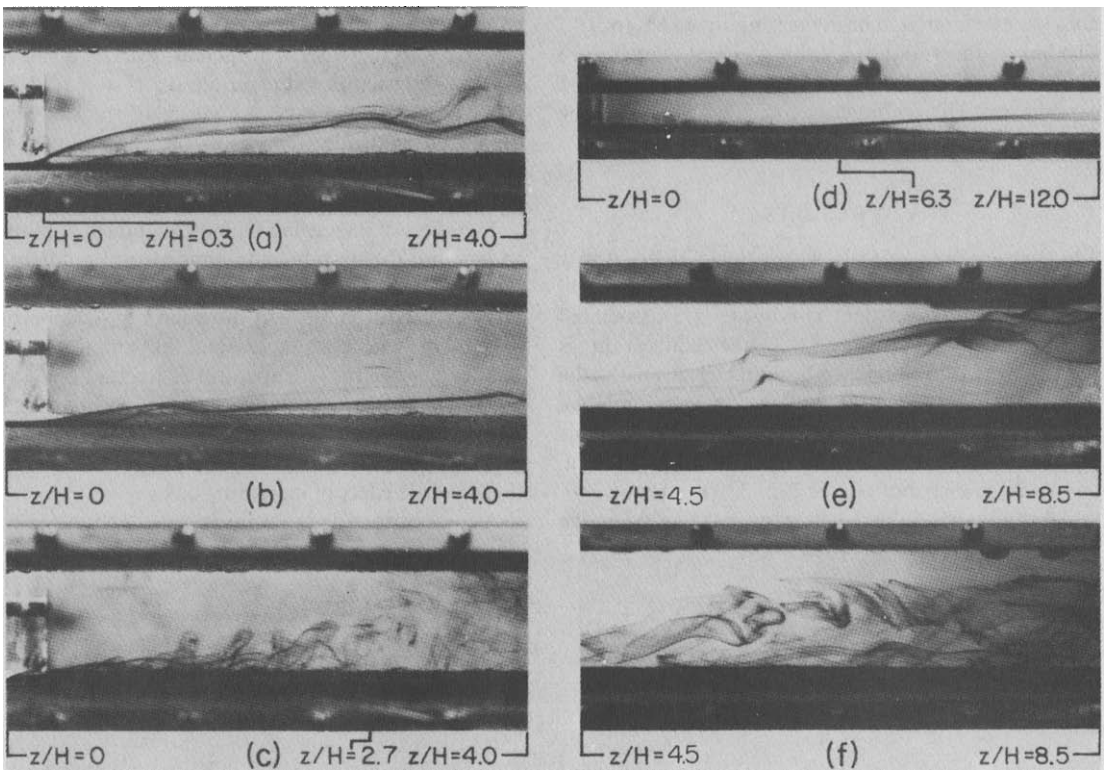

FIG. 5. Composite of dye-injection results for (a) $q_b = 1000$ W/m^2, $q_t = 0$, $w_m = 10$ mm/s, $H = 60$ mm ($Re_H = 650$, $Gr_{H,q} = 7.0 \times 10^7$); (b) $q_b = 1000$ W/m^2, $q_t = 0$, $w_m = 20$ mm/s, $H = 60$ mm ($Re_H = 1300$, $Gr_{H,q} = 7.0 \times 10^7$); (c) $q_b = 6000$ W/m^2, $q_t = 0$, $w_m = 10$ mm/s, $H = 60$ mm ($Re_H = 650$, $Gr_{H,q} = 4.2 \times 10^8$); (d) $q_b = 1000$ W/m^2, $q_t = 0$, $w_m = 30$ mm/s, $H = 20$ mm ($Re_H = 650$), $Gr_{H,q} = 8.6 \times 10^5$); (e) $q_b = 1000$ W/m^2, $q_t = 0$, $w_m = 10$ mm/s, $H = 60$ mm ($Re_H = 650$, $Gr_{H,q} = 7.0 \times 10^7$); (f) $q_b = 1000$ W/m^2, $q_t = 6000$ W/m^2, $w_m = 10$ mm/s, $H = 60$ mm ($Re_H = 650$, $Gr_{H,q} = 7.0 \times 10^7$).

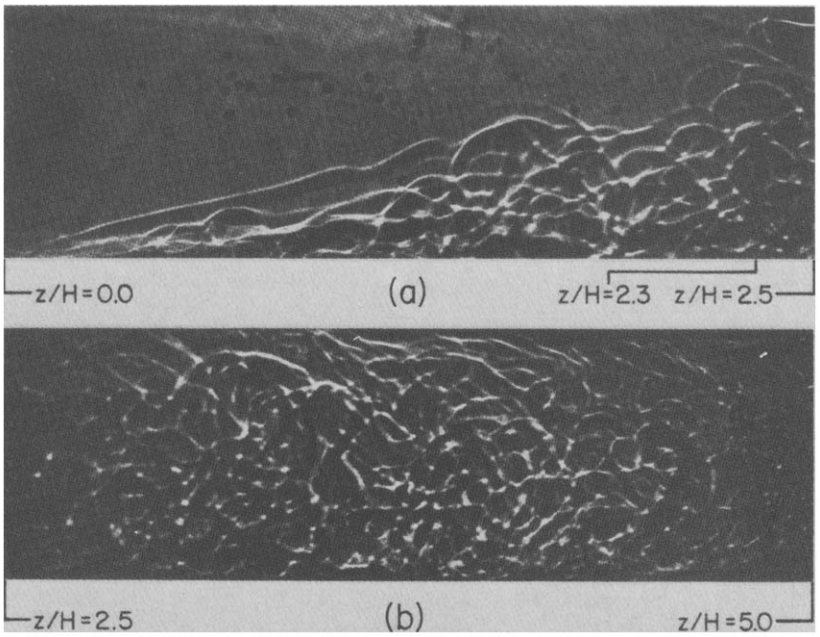

FIG. 6. Shadowgraphs for $q_b = 6000\,\mathrm{W/m^2}, q_t = 0, w_m = 10\,\mathrm{mm/s}, H = 60\,\mathrm{mm}$ ($Re_H = 650, Gr_{H,q} = 4.2 \times 10^8$).

the secondary flow is shown in Figs 6 and 7. In Fig. 6 penetration to the top surface occurs at $z/H \approx 2.3$; in Fig. 7 it occurs at $z/H \approx 3.8$. The effect of $Gr_{H,q}$ is shown in Figs 6 and 8. With decreasing $Gr_{H,q}$, mixing associated with the buoyancy induced flow is less intense and vertical penetration of the flow is delayed.

The flow visualization results were used to correlate onset and vertical penetration of the buoyancy driven flow in terms of the mixed convection parameter $Ra_{H,q}^{3/4}/Gz_H$, which is developed in Section 3.3. Onset of the flow corresponds to a parameter value of approximately 200, while penetration of the secondary flow to the top plate (or to the bottom of the stabilized layer for $q_t > 0$) occurs for parameter values in excess of approximately 5000.

3.2 *Top plate heat transfer measurements*

The foregoing flow visualization results suggest that, for the conditions of this study, the top plate thermal boundary layer is sufficiently stratified to resist significant penetration by buoyancy driven flows originating from the bottom plate. Hence bottom

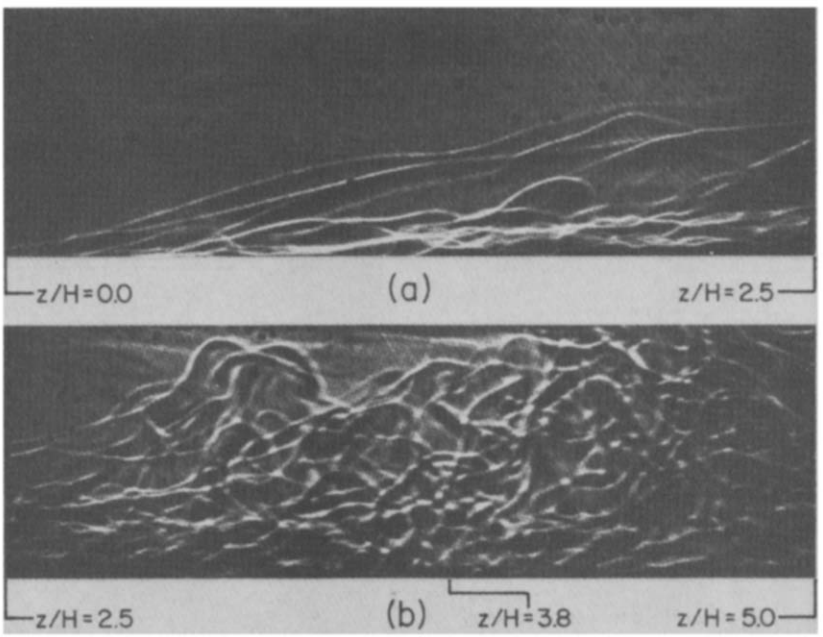

FIG. 7. Shadowgraphs for $q_b = 6000\ \mathrm{W/m^2}$, $q_t = 0$, $w_m = 20$ mm/s, $H = 60$ mm ($Re_H = 1300$, $Gr_{H,q} = 4.2 \times 10^8$).

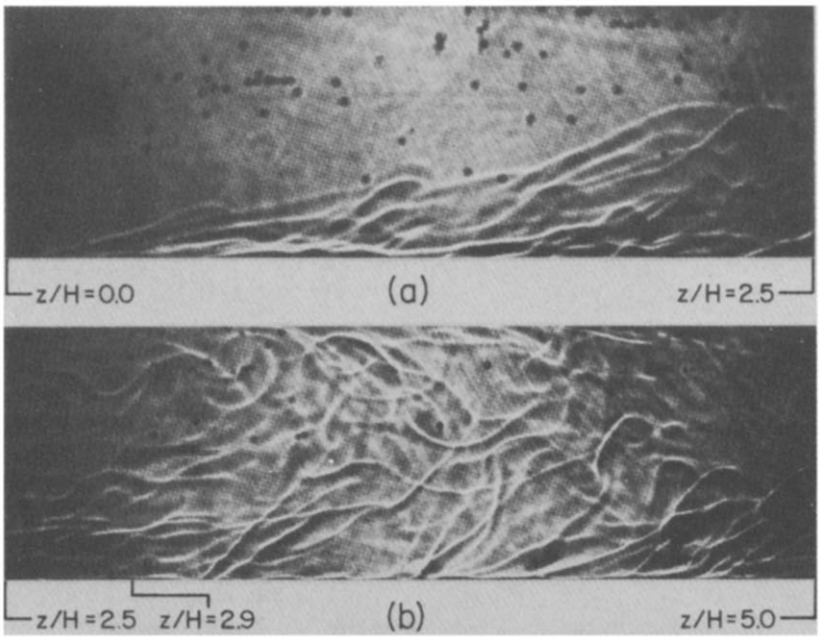

FIG. 8. Shadowgraphs for $q_b = 2000\,W/m^2, q_t = 0, w_m = 10\,mm/s, H = 60\,mm$ ($Re_H = 650, Gr_{H,q} = 1.4 \times 10^8$).

heating should have a negligible effect on top plate boundary layer conditions, which should then be dominated by forced convection. It is therefore reasonable to compare top plate heat transfer data with predictions for forced convection between parallel plates. Such a comparison is made in Fig. 9(a) where predictions are based on an exact solution for hydrodynamically developed laminar flow with $q_b = q_t$ [25]. The agreement is good, except for $z/H < 4$, where the data are influenced by longitudinal conduction within the plate. The effect, which is much more pronounced for the top plate than for the bottom plate, increases upstream values of T_t, thereby reducing experimental values of $Nu_{H,t}$. Figure 9(b) reveals the extent to which data are underpredicted by the laminar model when flow conditions are transitional (the Reynolds number exceeds the critical value of $Re_{H,c} \approx 1400$ [28]).

Top plate heat transfer data were approximately independent of q_t over the range $q_t \leqslant 6000\,W/m^2$ and weakly dependent on q_b/q_t over the range $0 \leqslant q_b/q_t \leqslant 2$. This dependence is attributed more to the influence of q_b on T_m than to the effect of the buoyancy driven flow. With increasing q_b/q_t, T_m may increase faster than T_t, causing $(T_t - T_m)$ to decrease and $Nu_{H,t}$ to increase. The effect is well known for annular flows [26] and has been predicted from a finite-difference solution for laminar, forced convection between parallel plates [29]. It increases with increasing q_b/q_t, increasing z/H and decreasing Re_H.

All of the top plate heat transfer data are plotted in Fig. 10, along with the forced convection correlation

$$Nu_H = 1.183 Gz_H^{1/3} \tag{3}$$

proposed by Shah [30] for $q_b/q_t = 1$. Although the comparison is affected by experimental uncertainties

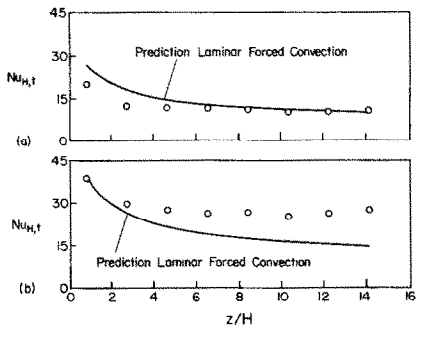

FIG. 9. Comparison of top plate heat transfer data for $q_t = q_b = 1000\,W/m^2$ and $H = 60$ mm with predictions for laminar and transitional forced convection: (a) $Re_H = 1300$, (b) $Re_H = 3900$.

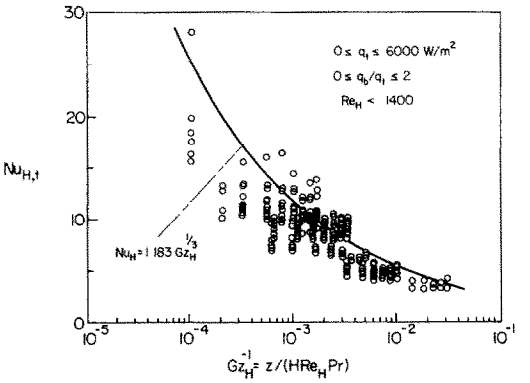

FIG. 10. Comparison of top plate data with forced convection heat transfer correlation.

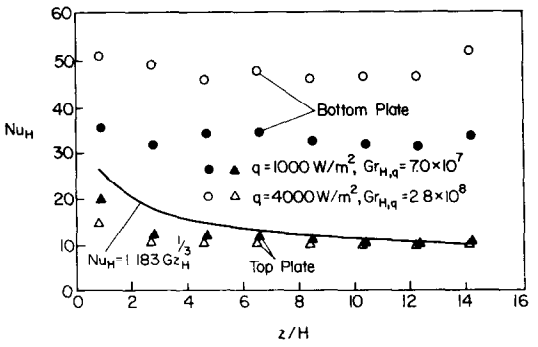

FIG. 11. Comparison of top and bottom plate heat transfer measurements for $H = 60$ mm, $Re_H = 1300$ and $q_t = q_b$.

and plate conduction in the entrance region, the agreement is reasonable and is consistent with the premise that top plate heat transfer is not significantly influenced by bottom plate buoyancy effects.

It should be noted that additional experiments performed at very low Reynolds number ($Re_H \approx 70$) yielded top plate Nusselt numbers which were three to four times less than results for pure forced convection. Use of flow visualization to investigate this behavior revealed a region of weak recirculating flow near the top plate, which is similar to flows observed by Kennedy and Zebib [23, 31] and Luikov *et al.* [32] due to heating from above.

3.3 *Bottom plate heat transfer measurements*

Although small for the top plate, free convection effects are significant at the bottom plate. Buoyancy induced motion for $Ra_{H,q}^{3/4}/Gz_H > 200$ causes the laminar flow to become random (possibly turbulent), with a significant increase in the convection coefficient. This behavior is shown in Fig. 11, where the bottom plate Nusselt number is much larger than that at the top plate for symmetrical heating ($q_t = q_b$). Moreover, $Nu_{H,t}$ is independent of the heat flux and well predicted by the forced convection correlation, while $Nu_{H,b}$ increases by approximately 50% for a 4-fold increase in heat flux and is significantly underpredicted by the forced convection correlation. Concerning the effect of buoyancy on heat transfer enhancement at the bottom plate, results from other experiments are summarized in Table 1 and reveal increased enhancement with increasing z/H, H and q_b, as well as with decreasing w_m. Absence of a significant decay in $Nu_{H,b}$ for the entrance region data of Fig. 11 is attributed to heat transfer enhancement by the buoyancy-driven flow.

Table 1. Influence of free convection on mixed convection heat transfer from the bottom plate

z/H	$Nu_{H,b}/Nu_{H,F}$		% Change
	$w_m = 10$ mm/s	20 mm/s	
2.7	2.17	1.86	−14
13.8	4.14	3.38	−18
	$q_b = 1000$ W/m²	6000 W/m²	
2.7	2.34	3.55	52
13.8	3.93	6.68	70
	$H = 20$ mm	60 mm	
2.7	0.94	2.90	208
13.8	1.78	5.76	224

In the early stages of this work it was thought that the stable layer induced by heating from above could diminish $Nu_{H,b}$ by inhibiting the buoyancy driven flow. However, the flow visualization results suggested that, even with a strongly stratified upper layer, lower fluid layers remained well mixed, in which case $Nu_{H,b}$ should not decrease with increasing q_t. This conclusion is consistent with the data of Fig. 12, which, in fact, reveal the opposite trend. The increase in $Nu_{H,b}$ with increasing q_t/q_b is attributed to the effect of q_t on T_m. This effect is much more pronounced for the bottom plate data than for either the top plate data or predictions based on pure forced convection. Differences in the effect are due to the significant reduction in T_b caused by the buoyancy driven flow. This reduction enhances the effect of increasing T_m on the value of $(T_b - T_m)$. The worst case condition of this study corresponds to $q_t/q_b = 6$ and $H = 20$ mm (Fig. 12b), where $Nu_{H,b}$ approaches infinity for $z/H \approx 20$ and is negative for $z/H > 20$. Although discernable, the effect of q_t/q_b on $Nu_{H,b}$ remained small (<10%) for $q_t/q_b < 2$.

A major objective of this study was to develop a reliable correlation for mixed convection heat transfer from the bottom plate of a horizontal, parallel plate channel. Initially, efforts were made to correlate data in terms of Grashof to Reynolds number ratios of the form Gr_L/Re_L^n, where n was assigned customary values for mixed convection flows (3/2, 2, or 5/2), L was set equal to z or H, and Gr_L was based on ΔT_b or q_b. All such efforts were unsuccessful, however, and subsequent attempts involved use of a correlation suggested by Acrivos [33] and Churchill [34], which involves the

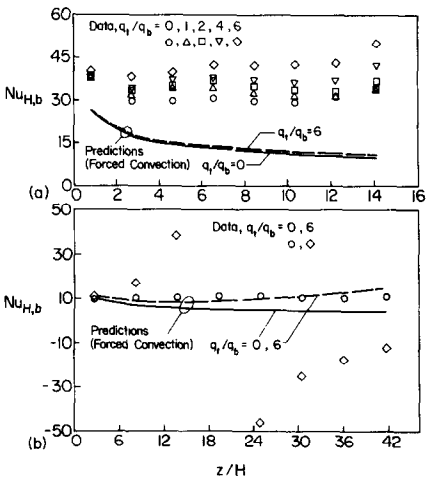

FIG. 12. Effect of heat flux ratio on bottom plate Nusselt number for $q_b = 1000$ W/m²: (a) $H = 60$ mm, $Re_H = 1300$, $Gr_{H,q} = 7.0 \times 10^7$, (b) $H = 20$ mm, $Re_H = 217$, $Gr_{H,q} = 8.6 \times 10^5$.

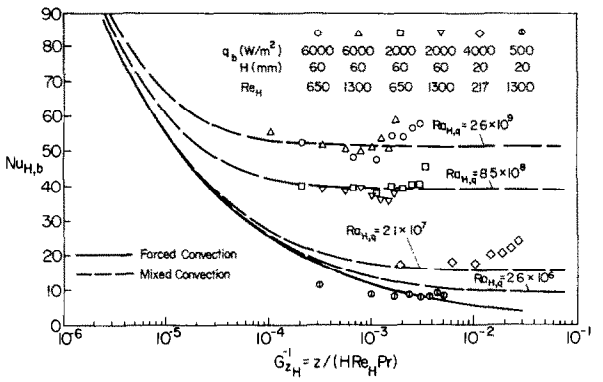

FIG. 13. Comparison of data with forced and mixed convection correlations for the bottom plate Nusselt number ($q_t = q_b$).

following superposition of results for pure forced (F) and natural (N) convection.

$$Nu^n = Nu_F^n + Nu_N^n \tag{4}$$

The power n is chosen to provide the best correlation, and a value of 3 was found to be most appropriate for the conditions of this study. Equation (3), which was developed for laminar, forced convection between parallel plates with uniform heat flux, was used for the pure forced convection component of equation (4). For the pure natural convection component, the correlation of Fujii and Imura [35] for turbulent-free convection from a heated horizontal plate (facing upward) was used.

$$Nu_{H,N} = 0.14\, Ra_H^{1/3} \tag{5}$$

However, since the surface condition of this study is one of uniform heat flux, the substitution $Ra_H = Ra_{H,q}/Nu_H$ is made, and the correlation is of the form

$$Nu_{H,N} = 0.229\, Ra_{H,q}^{1/4} \tag{6}$$

Substituting equations (3) and (6) into equation (4) and using $n = 3$, the correlation for mixed convection from the bottom plate of a parallel plate channel is

$$Nu_H = [1.656\, Gz_H + 0.012\, Ra_{H,q}^{3/4}]^{1/3} \tag{7}$$

or, dividing by equation (3), the ratio of the mixed convection to the forced convection Nusselt number is

$$\frac{Nu_H}{Nu_{H,F}} = [1 + 0.0073(Ra_{H,q}^{3/4}/Gz_H)]^{1/3} \tag{8}$$

From equation (7), the Nusselt number may be plotted as a function of the reciprocal Graetz number for different values of the Rayleigh number. This is done in Fig. 13 for four values of $Ra_{H,q}$ corresponding to the data of the figure. Agreement between the mixed and forced convection correlations improves with increasing Gz_H, and decreasing $Ra_{H,q}$, and for the smallest value of $Ra_{H,q}$ the data are in reasonable agreement with the correlations for all but the first station. Overprediction of the measured result at this station is attributed to plate axial conduction, which is most pronounced in the forced convection limit. Agreement of the mixed convection correlation with data for the three larger values of $Ra_{H,q}$ is good at all but downstream measurement stations for which the effect of q_t on T_m becomes discernible.

The form of equation (8) suggests that all data should collapse to a single curve if plotted as $Nu_{H,b}/Nu_{H,F}$ versus $Ra_{H,q}^{3/4}/Gz_H$. Figures 14 through 16, in which all of the data have been plotted for $q_t/q_b = 0$, 1 and 2, respectively, reveal that this is in fact the case. The top plate heat flux has only a small effect on $Nu_{H,b}$, and there is good agreement between the data and the correlation. In Fig. 14 all data are correlated within 38%, and 77% of the data are correlated within 10%. In

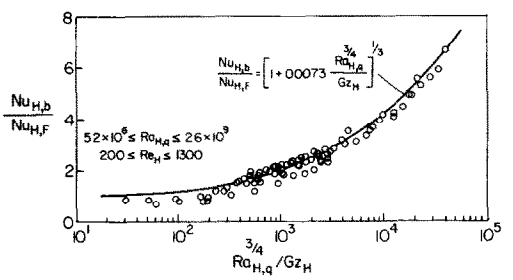

FIG. 14. Correlation of bottom plate Nusselt number data for $q_t/q_b = 0$.

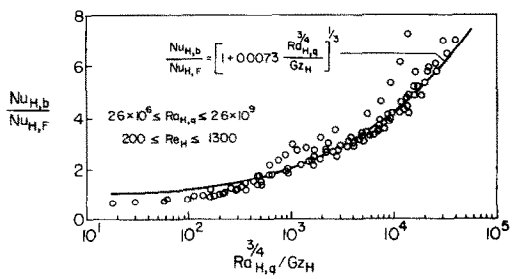

FIG. 15. Correlation of bottom plate Nusselt number data for $q_t/q_b = 1$.

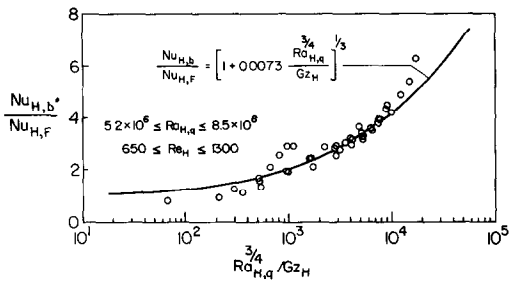

FIG. 16. Correlation of bottom plate Nusselt number data for $q_t/q_b = 2$.

Figs. 15 and 16, all data are correlated within 48% and 72% of the data are correlated within 10%. For $q_t/q_b > 2$, differences between the data and the correlation become significant and, by itself, $Ra_{H,q}^{3/4}/Gz_H$ is not a proper correlating parameter. As shown in Fig. 17 for $q_t/q_b = 6$, the data are significantly underpredicted due to the effect of q_t on T_m.

The foregoing correlations may be used to delineate regions of forced, mixed and free convection for the bottom plate. If the transition from laminar, forced convection to mixed convection is said to occur when $Nu_H/Nu_{H,F}$ exceeds 1.1, equation (8) suggests mixed convection conditions for $(Ra_{H,q}^{3/4}/Gz_H) > 45$. This value is less than the result of 200 inferred from flow visualization. If transition from mixed convection to turbulent free convection is said to occur when $Nu_H/Nu_{H,N}$ becomes less than 1.1, equations (6) and (7) suggest pure free convection for $(Ra_{H,q}^{3/4}/Gz_H) > 417$. This value is substantially less than the flow visualization result of approximately 5000 for the establishment of complete mixing.

4. SUMMARY

Experiments have been performed to determine the effects of free convection on laminar, forced convection flow between horizontal parallel plates which are symmetrically and asymmetrically heated. Major conclusions are as follows.

(1) Flow at the top plate is characterized by a laminar, forced convection boundary layer. Thermal stratification within this layer inhibits the penetration of buoyancy driven flows from the bottom plate, and, for the conditions of this study, bottom heating has little effect on top plate conditions.

(2) Conditions at the bottom plate are independent of top plate heating but are strongly influenced by a buoyancy induced flow whose effects increase with increasing q_b, H and z and decreasing w_m. From flow visualization, onset of the buoyancy driven flow is observed to occur for $Ra_{H,q}^{3/4}/Gz_H \approx 200$ and attendant mixing effects penetrate to all but the top stable layer for $Ra_{H,q}^{3/4}/Gz_H \approx 5000$.

(3) Heat transfer at the bottom plate is significantly enhanced by the buoyancy driven flow, with mixed convection coefficients exceeding those associated with pure forced convection by as much as a factor of seven. For $q_t/q_b \leqslant 2$, mixed convection heat transfer is well correlated by equation (7).

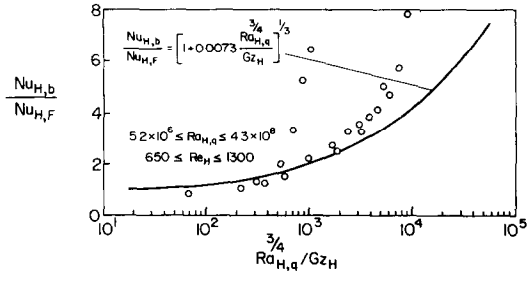

FIG. 17. Correlation of bottom plate Nusselt number data for $q_t/q_b = 6$.

Acknowledgement—We are grateful for support of this work by the National Science Foundation under Grant No. MEA-8316580.

REFERENCES

1. S. T. McComas and E. R. G. Eckert, Combined free and forced convection in a horizontal circular tube, *Trans. Amer. Soc. Mech. Engrs, J. Heat Transfer* **88,** 147–153 (1966).
2. R. L. Shannon and C. A. Depew, Combined free and forced laminar convection in a horizontal tube with uniform heat flux, *Trans. Amer. Soc. Mech. Engrs, J. Heat Transfer* **90,** 353–359 (1968).
3. A. E. Bergles and R. R. Simonds, Combined forced and free convection for laminar flow in horizontal tubes with uniform heat flux, *Int. J. Heat Mass Transfer* **14,** 1989–2000 (1971).
4. S. M. Marcos and A. E. Bergles, Experimental investigation of combined forced and free laminar convection in horizontal tubes, *Trans. Amer. Soc. Mech. Engrs, J. Heat Transfer* **97,** 212–218 (1975).
5. J. A. Sabbagh, A. Aziz, A. S. El-Ariny and G. Hamad, Combined free and forced convection in circular tubes, *Trans. Amer. Soc. Mech. Engrs, J. Heat Transfer* **98,** 322–328 (1976).
6. E. del Casal and W. N. Gill, A note on natural convection effects in fully developed horizontal tube flow, *AIChE J.* **8,** 570–574 (1962).
7. G. N. Faris and R. Viskanta, An analysis of laminar combined forced and free convection heat transfer in a horizontal tube, *Int. J. Heat Mass Transfer* **12,** 1295–1303 (1969).
8. P. H. Newell and A. E. Bergles, Analysis of combined free and forced convection for fully developed laminar flow in horizontal tubes, *Trans. Amer. Soc. Mech. Engrs, J. Heat Transfer* **92,** 83–93 (1970).
9. S. V. Patankar, S. Ramadhyani and E. M. Sparrow, Effect of circumferentially nonuniform heating on laminar combined convection in a horizontal tube, *Trans. Amer. Soc. Mech. Engrs, J. Heat Transfer* **100,** 63–70 (1978).
10. L. S. Yao, Free-forced convection in the entry region of a heated straight pipe, *Trans. Amer. Soc. Mech. Engrs, J. Heat Transfer* **100,** 212–218 (1978).
11. C. A. Hieber, Laminar mixed convection in an isothermal horizontal tube: correlation of heat transfer data, *Int. J. Heat Mass Transfer* **25,** 1737–1746 (1982).
12. Y. Mori and Y. Uchida, Forced convection heat transfer between horizontal flat plates, *Int. J. Heat Mass Transfer* **9,** 803–817 (1966).

13. M. Akiyama, G. J. Hwang and K. C. Cheng, Experiments on the onset of longitudinal vortices in laminar forced convection between horizontal plates, *Trans. Amer. Soc. Mech. Engrs, J. Heat Transfer* **93,** 335–341 (1971).
14. S. Ostrach and Y. Kamotani, Heat transfer augmentation in laminar fully developed channel flow by means of heating from below, *Trans. Amer. Soc. Mech. Engrs, J. Heat Transfer* **97,** 220–225 (1975).
15. G. J. Hwang and C. L. Liu, An experimental study of convection instability in the thermal entrance region of a horizontal parallel-plate channel heated from below, *Canadian J. Chem. Eng.* **54,** 521–525 (1976).
16. Y. Kamotani and S. Ostrach, Effect of thermal instability on thermally developing laminar channel flow, *Trans. Amer. Soc. Mech. Engrs, J. Heat Transfer* **98,** 62–66 (1976).
17. Y. Kamotani, S. Ostrach and H. Miao, Convective heat transfer augmentation in thermal entrance regions by means of thermal instability, *Trans. Amer. Soc. Mech. Engrs, J. Heat Transfer* **101,** 222–226 (1979).
18. K. C. Cheng and G. J. Hwang, Numerical solution for combined free and forced laminar convection in horizontal rectangular channels, *Trans. Amer. Soc. Mech. Engrs, J. Heat Transfer* **91,** 59–66 (1969).
19. W. Nakayama, G. J. Hwang and K. C. Cheng, Thermal instability in planar Poiseuille flow, *Trans. Amer. Soc. Mech. Engrs, J. Heat Transfer* **92,** 61–67 (1970).
20. K. C. Cheng, S. W. Hong and G. J. Hwang, Buoyancy effects on laminar heat transfer in the thermal entrance region of horizontal rectangular channels with uniform wall heat flux for large Prandtl number fluid, *Int. J. Heat Mass Transfer* **15,** 1819–1827 (1972).
21. G. J. Hwang and K. C. Cheng, Convection instability in the thermal entrance region of a horizontal parallel-plate channel heated from below, *Trans. Amer. Soc. Mech. Engrs, J. Heat Transfer* **95,** 72–78 (1973).
22. T. V. Nguyen, I. L. Maclaine-Cross and G. deVahl Davis, Combined forced and free convection between parallel plates, *Numerical Methods in Thermal Problems* (edited by R. W. Lewis and K. Morgan) pp. 269–278, Pine Ridge Press, U.K. (1979).
23. K. J. Kennedy and A. Zebib, Combined free and forced convection between horizontal parallel planes: some case studies, *Int. J. Heat Mass Transfer* **26,** 471–478 (1983).
24. M. M. M. Abou-Ellail and S. M. Morcos, Buoyancy effects in the entrance region of horizontal rectangular channels, *Trans. Amer. Soc. Mech. Engrs, J. Heat Transfer* **105,** 924–927 (1983).
25. R. K. Shah and A. L. London, *Laminar Forced Convection in Ducts*, Academic Press, New York (1978).
26. W. M. Kays, *Convective Heat and Mass Transfer*, McGraw-Hill, New York (1976).
27. S. J. Kline and F. A. McClintock, Describing uncertainties in single-sample experiments, *Amer. Soc. Mech. Engrs, Mechanical Engineering* **75,** 3–8 (1953).
28. R. W. Fox and A. T. McDonald, *Introduction to Fluid Mechanics*, John Wiley, New York (1978).
29. D. G. Osborne, Combined convection heat transfer for water flow between horizontal parallel plates with constant heat fluxes, MSME Thesis, Purdue University, W. Lafayette, Indiana (1983).
30. R. K. Shah, Thermal entry length solutions for the circular tube and parallel plates, *Proc. Third Natl. Heat Mass Transfer Conf.*, Indian Inst. Tech., Bombay, Vol. I, Paper No. HMT-11-75.
31. K. J. Kennedy and A. Zebib, Combined forced and free convection between parallel plates, Paper 82-IHTC-152, *Proc. 7th Int. Heat Transfer Conference*, Hemisphere Publishing Co., New York, Vol. 3, pp. 447–453 (1982).
32. A. V. Luikov, B. M. Berkovskii and V. E. Fertman, Stimulation of free convection by heating from above, *Progress in Heat and Mass Transfer*. Vol. 2, Pergamon Press, Oxford, pp. 77–89 (1969).
33. A. Acrivos, On the combined effect of forced and free convection heat transfer in laminar boundary layer flows, *Chem. Eng. Science* **21,** 343–349 (1966).
34. S. W. Churchill, A comprehensive correlating equation for laminar, assisting, forced and free convection, *AIChE J.* **23,** 10–16 (1977).
35. T. Fujii and H. Imura, Natural convection heat transfer from a plate with arbitrary inclination, *Int. J. Heat Mass Transfer* **15,** 755–767 (1972).

CONVECTION THERMIQUE MIXTE, LAMINAIRE POUR UN ECOULEMENT ENTRE PLAQUES PARALLELES, HORIZONTALES AVEC CHAUFFAGE DISSYMETRIQUE

Résumé—Une étude expérimentale détermine les conditions hydrodynamiques et thermiques dans un écoulement laminaire d'eau entre plaques parallèles, horizontales avec des flux thermiques uniformes différents. La visualisation de l'écoulement et les mesures de température revèlent l'existence d'une convection naturelle qui influence fortement les conditions sur la plaque inférieure, mais qui a une faible influence sur les conditions à la plaque supérieure. Le transfert thermique à la plaque supérieure est dominé par la convection forcée, tandis qu'à la plaque inférieure agit une convection mixte et il peut être représenté en fonction du paramètre $Ra_{H,q}^{3/4}/Gz_H$ pour un rapport de flux inférieur à 2 entre sommet et base. Pour le domaine de flux thermique considéré, les conditions d'écoulement aux plaques supérieure et inférieure sont indépendantes du flux thermique sur la plaque opposée.

WÄRMEÜBERGANG BEI LAMINARER MISCHKONVEKTION IN STRÖMUNGEN ZWISCHEN HORIZONTALEN PARALLELEN PLATTEN MIT ASYMMETRISCHER BEHEIZUNG

Zusammenfassung—Das hydrodynamische und thermische Verhalten einer laminaren Strömung von Wasser zwischen zwei horizontalen parallelen Platten mit gleichförmiger asymmetrischer Verteilung der Wärmestromdichte wurde experimentell untersucht. Die Beobachtung der Strömung und Temperaturmessungen zeigen die Existenz einer Auftriebsströmung, die einen großen Einfluß auf die Bedingungen an der unteren Platte, aber nur geringen Einfluß auf die Bedingungen an der oberen Platte hat. Der Wärmeübergang an der oberen Platte wird durch erzwungene Konvektion bestimmt, während der Wärmeübergang an der unteren Platte durch Mischkonvektion charakterisiert ist. Für eine Wärmestromdichte kleiner 2 von der oberen zur unteren Platte kann der Wärmeübergang in Abhängigkeit von $Ra_{H,q}^{3/4}/Gz_H$ korreliert werden. Im betrachteten Bereich der Wärmestromdichte sind die Strömungsbedingungen an der oberen und unteren Platte unabhängig von der Wärmestromdichte an der jeweils gegenüberliegenden Platte.

ЛАМИНАРНЫЙ ТЕПЛОПЕРЕНОС СМЕШАННОЙ КОНВЕКЦИЕЙ ДЛЯ ТЕЧЕНИЯ МЕЖДУ АСИММЕТРИЧНО НАГРЕВАЕМЫМИ ГОРИЗОНТАЛЬНЫМИ ПАРАЛЛЕЛЬНЫМИ ПЛАСТИНАМИ

Аннотация—Экспериментально изучены гидродинамические и тепловые режимы при ламинарном течении воды между горизонтальными параллельными пластинами с однородными асимметричными тепловыми потоками. Визуальное изучение течения и измерения температуры указали на существование вторичного течения, вызванного подъемными силами, которое оказывает сильное влияние на режим у нижней, но слабо влияет на режим у верхней пластины. Теплоперенос у верхней пластины обусловлен вынужденной конвекцией, в то время как у нижней характеризуется смешанной конвекцией и отношение верхнего и нижнего потоков, выраженное через параметр $Ra_{H,q}^{3/4}/Gz_H$, меньше 2. Для диапазона рассмотренных тепловых потоков режимы течения у верхней и нижней пластин не зависят от теплового потока у противоположной пластины.